

IMAGE DECONVOLUTION UNDER POISSON NOISE USING SPARSE REPRESENTATIONS AND PROXIMAL THRESHOLDING ITERATION

F.-X. Dupé^a, M.J. Fadili^a and J.-L. Starck^b

^a GREYC UMR CNRS 6072 ^b DAPNIA/SEDI-SAP CEA-Saclay
14050 Caen France 91191 Gif-sur-Yvette France

ABSTRACT

We propose an image deconvolution algorithm when the data is contaminated by Poisson noise. The image to restore is assumed to be sparsely represented in a dictionary of waveforms such as the wavelet or curvelet transform. Our key innovations are: First, we handle the Poisson noise properly by using the Anscombe variance stabilizing transform leading to a *non-linear* degradation equation with additive Gaussian noise. Second, the deconvolution problem is formulated as the minimization of a convex functional with a data-fidelity term reflecting the noise properties, and a non-smooth sparsity-promoting penalties over the image representation coefficients (e.g. ℓ_1 -norm). Third, a fast iterative backward-forward splitting algorithm is proposed to solve the minimization problem. We derive existence and uniqueness conditions of the solution, and establish convergence of the iterative algorithm. Experimental results are carried out to show the striking benefits gained from taking into account the Poisson statistics of the noise. These results also suggest that using sparse-domain regularization may be tractable in many deconvolution applications, e.g. astronomy or microscopy.

Index Terms— Deconvolution, Poisson noise, Proximal iteration, forward-backward splitting, Iterative thresholding, Sparse representations.

1. INTRODUCTION

Deconvolution is a longstanding problem in many areas of signal and image processing (e.g. biomedical imaging [1], astronomy [2], remote-sensing, to quote a few). For example, research in astronomical image deconvolution has recently seen considerable work, partly triggered by the Hubble space telescope (HST) optical aberration problem at the beginning of its mission. In biomedical imaging, researchers are also increasingly relying on deconvolution to improve the quality of images acquired by confocal microscopes. Deconvolution may then prove crucial for exploiting images and extracting scientific content.

There is an extensive literature on deconvolution problems. One might refer to well-known dedicated monographs on the subject. In presence of Poisson noise, several deconvolution methods have been proposed such as Tikhonov-Miller inverse filter and Richardson-Lucy (RL) algorithms; see [1, 2] for an excellent review. The RL has been used extensively in applications because it is adapted to Poisson noise. The RL algorithm, however, amplifies noise after a few iterations, which can be avoided by introducing regularization. In [3], the authors presented a Total Variation (TV)-regularized RL algorithm, and Starck et al. advocated a wavelet-regularized RL algorithm [2].

In the context of deconvolution with gaussian white noise, sparsity-promoting regularization over orthogonal wavelet coefficients has been recently proposed [4, 5]. Generalization to frames was proposed in [6, 7]. In [8], the authors presented an image deconvolution algorithm by iterative thresholding in an overcomplete dictionary of transforms. However, all sparsity-based approaches published so far have mainly focused on Gaussian noise.

In this paper, we propose an image deconvolution algorithm for data blurred and contaminated by Poisson noise. The Poisson noise is handled properly by using the Anscombe VST, leading to a *non-linear* degradation equation with additive Gaussian noise, see (2). To regularize the solution, we impose a sparsity prior on the representation coefficients of the image to restore, e.g. wavelet or curvelet coefficients. Then, the deconvolution problem is formulated as the minimization of a convex functional with a data-fidelity term reflecting the noise properties, and a non-smooth sparsity-promoting penalties over the image representation coefficients. Inspired by the work in [5], a fast proximal iterative algorithm is proposed to solve the minimization problem. We also provide an analysis of the optimization problem and establish convergence of the iterative algorithm. Experimental results are carried out to compare our approach and show the striking benefits gained from taking into account the Poisson nature of the noise.

Notation

Let \mathcal{H} a real Hilbert space, here a finite dimensional vector subspace of \mathbb{R}^n . We denote by $\|\cdot\|_2$ the norm associated with the inner product in \mathcal{H} , and \mathbf{I} is the identity operator on \mathcal{H} . x and α are respectively reordered vectors of image samples and transform coefficients. A function f is proper if it is not identically $+\infty$ everywhere. A function f is coercive, if $\lim_{\|x\|_2 \rightarrow +\infty} f(x) = +\infty$. $\Gamma_0(\mathcal{H})$ is the class of all proper lower semi-continuous convex functions from \mathcal{H} to $]-\infty, +\infty]$. The subdifferential of f is denoted ∂f .

2. PROBLEM STATEMENT

Consider the image formation model where an input image x is blurred by a point spread function (PSF) h and contaminated by Poisson noise. The observed image is then a discrete collection of counts $y = (y_i)_{1 \leq i \leq n}$ where n is the number of samples. Each count y_i is a realization of an independent Poisson random variable with a mean $(h \otimes x)_i$, where \otimes is the circular convolution operator. Formally, this writes $y_i \sim \mathcal{P}((h \otimes x)_i)$.

A naive solution to this deconvolution problem would be to apply traditional approaches designed for Gaussian noise. But

this would be awkward as (i) the noise tends to Gaussian only for large mean $(h \otimes x)_i$ (central limit theorem), and (ii) the noise variance depends on the mean anyway. A more adapted way would be to adopt a bayesian framework with an adapted anti-log-likelihood score reflecting the Poisson statistics of the noise. Unfortunately, doing so, we would end-up with a functional which does not satisfy some key properties (the Lipschitzian property in [5]), hence preventing us from using the backward-forward splitting proximal algorithm to solve the optimization problem. To circumvent this difficulty, we propose to handle the noise statistical properties by using the Anscombe VST defined as

$$z_i = 2\sqrt{y_i + \frac{3}{8}}, \quad 1 \leq i \leq n. \quad (1)$$

Some previous authors [9] have already suggested to use the Anscombe VST, and then deconvolve with wavelet-domain regularization as if the stabilized observation z_i were linearly degraded by h and contaminated by additive Gaussian noise. But this is not valid as standard asymptotic results of the Anscombe VST state that

$$z_i = 2\sqrt{(h \otimes x)_i + \frac{3}{8}} + \varepsilon, \quad \varepsilon \sim \mathcal{N}(0, 1) \quad (2)$$

where ε is an additive white Gaussian noise of unit variance. In words, z is *non-linearly* related to x . In Section 4.1, we provide an elegant optimization problem and a fixed point algorithm taking into account such a non-linearity.

3. SPARSE IMAGE REPRESENTATION

Let $x \in \mathcal{H}$ be an $\sqrt{n} \times \sqrt{n}$ image. x can be written as the superposition of elementary atoms φ_γ parameterized by $\gamma \in \mathcal{I}$ such that:

$$x = \sum_{\gamma \in \mathcal{I}} \alpha_\gamma \varphi_\gamma = \Phi \alpha, \quad |\mathcal{I}| = L \quad (3)$$

We denote by Φ the dictionary i.e. the $n \times L$ matrix whose columns are the generating waveforms $(\varphi_\gamma)_{\gamma \in \mathcal{I}}$ all normalized to a unit ℓ_2 -norm. The forward transform is then defined by a non-necessarily square matrix $\mathbf{T} = \Phi^T \in \mathbb{R}^{L \times n}$ with $L \geq n$. When $L > n$ the dictionary is said to be redundant or over-complete. In the case of the simple orthogonal basis, the inverse transform is trivially $\Phi = \mathbf{T}^T$. Whereas assuming that \mathbf{T} is a tight frame implies that the frame operator satisfies $\mathbf{T}^T \mathbf{T} = A \mathbf{I}$, where $A > 0$ is the tight frame constant. For tight frames, the pseudo-inverse reconstruction operator reduces to $A^{-1} \mathbf{T}$.

Our prior is that we are seeking for a good representation of x with only few significant coefficients. This makes sense since most practical signals or images are compressible in some transform domain (e.g. wavelets, curvelets, DCT, etc). These transforms generally correspond to an orthogonal basis or a tight frame. In the rest of the paper, Φ will be an orthobasis or a tight frame of \mathcal{H} .

4. SPARSE ITERATIVE DECONVOLUTION

We first define the notion of a proximity operator, which was introduced in [10] as a generalization of the notion of a convex projection operator.

Definition 1 (Moreau[10]). *Let $\varphi \in \Gamma_0(\mathcal{H})$. Then, for every $x \in \mathcal{H}$, the function $y \mapsto \varphi(y) + \|x - y\|^2 / 2$ achieves its infimum at a unique point denoted by $\text{prox}_\varphi x$. The operator $\text{prox}_\varphi : \mathcal{H} \rightarrow \mathcal{H}$ thus defined is the proximity operator of φ . We define the reflection operator $\text{rprox}_\varphi = 2 \text{prox}_\varphi - \mathbf{I}$.*

4.1. Optimization problem

The class of minimization problems we are interested in can be stated in the general form [5]:

$$\arg \min_{x \in \mathcal{H}} f_1(x) + f_2(x). \quad (4)$$

where $f_1 \in \Gamma_0(\mathcal{H})$, $f_2 \in \Gamma_0(\mathcal{H})$ and f_1 is differentiable with κ -Lipschitz gradient. We denote by \mathcal{M} the set of solutions. From (2) and (3), we immediately deduce the data fidelity term

$$F \circ H \circ \Phi(\alpha), \quad \text{with} \quad (5)$$

$$F : \eta \mapsto \sum_{i=1}^n f(\eta_i), \quad f(\eta_i) = \frac{1}{2} \left(z_i - 2\sqrt{\eta_i + \frac{3}{8}} \right)^2,$$

where H denotes the (block-Toeplitz) convolution operator. From a statistical perspective, (5) corresponds to the anti-log-likelihood score.

Adopting a bayesian framework and using a standard maximum a posteriori (MAP) rule, our goal is to minimize the following functional with respect to the representation coefficients α

$$(\mathbf{P}_{\lambda, \psi}) : \arg \min_{\alpha} J(\alpha) \quad (6)$$

$$J : \alpha \mapsto \underbrace{F \circ H \circ \Phi(\alpha)}_{f_1(\alpha)} + \underbrace{\iota_{\mathcal{C}} \circ \Phi(\alpha) + \lambda \sum_{i=1}^L \psi(\alpha_i)}_{f_2(\alpha)},$$

where we implicitly assumed that $(\alpha_i)_{1 \leq i \leq L}$ are independent and identically distributed with a Gibbsian density $\propto e^{-\lambda \psi(\alpha_i)}$. Notice that f_2 is not smooth. The penalty function ψ is chosen to enforce sparsity, $\lambda > 0$ is a regularization parameter and $\iota_{\mathcal{C}}$ is the indicator function of a convex set \mathcal{C} . In our case, \mathcal{C} is the positive orthant. We remind that the positivity constraint is because we are fitting Poisson intensities, which are positive by nature. We have the following,

Proposition 1.

- f_1 is convex function. It is strictly convex if Φ is an ortho-basis and $\ker(H) = \emptyset$ (i.e. the spectrum of the PSF does not vanish).
- f_1 is continuously differentiable with a κ -Lipschitz gradient where

$$\kappa \leq \left(\frac{2}{3}\right)^{3/2} 4A \|H\|_2^2 \|z\|_\infty < +\infty. \quad (7)$$

- $(\mathbf{P}_{\lambda, \psi})$ is a particular case of problem (4).

4.1.1. Characterization of the solution

Proposition 2. *Since J is coercive and convex, the following holds:*

1. *Existence:* $(\mathbf{P}_{\lambda, \psi})$ has at least one solution, i.e. $\mathcal{M} \neq \emptyset$.
2. *Uniqueness:* $(\mathbf{P}_{\lambda, \psi})$ has a unique solution if Φ is a basis and $\ker(H) = \emptyset$, or if ψ is strictly convex.

Proof: The existence is obvious because J is coercive. If Φ is an ortho-basis and $\ker(H) = \emptyset$ then f_1 is strictly convex and so is J leading to a strict minimum. Similarly, if ψ is strictly convex, so is f_2 , hence J . ■

4.1.2. Proximal iteration

For notational simplicity, we denote by Ψ the function $\alpha \mapsto \sum_i \psi(\alpha_i)$. The following useful lemmas are first stated:

Lemma 1. *The gradient of ∇f_1 is*

$$\nabla f_1(\alpha) = \Phi^T \circ H^* \circ \nabla F \circ H \circ \Phi(\alpha) \quad (8)$$

with

$$\nabla F(\eta) = \left(\frac{-z_i}{\sqrt{\eta_i + 3/8}} + 2 \right)_{1 \leq i \leq n} \quad (9)$$

The proof is straightforward.

Lemma 2. *Let Φ an orthobasis or a tight frame with constant c .*

1. *If $\alpha \in \mathcal{C}'$ then $\text{prox}_{f_2}(\alpha) = \text{prox}_{\lambda\Psi}(\alpha)$, $\mathcal{C}' = \{\alpha | \Phi\alpha \in \mathcal{C}\}$.*
2. *Otherwise, let $\sum_t \nu_t(1 - \nu_t) = +\infty$. Take $\gamma^0 \in \mathcal{H}$, and define the sequence of iterates:*

$$\gamma^{t+1} = \gamma^t + \nu_t \left(\text{rprox}_{\lambda\Psi + \frac{1}{2}\|\cdot - \alpha\|^2} \circ \text{rprox}_{\mathcal{C}'}(\gamma^t) \right) \quad (10)$$

where

$$\text{prox}_{\lambda\Psi + \frac{1}{2}\|\cdot - \alpha\|^2}(\gamma^t) = \left(\text{prox}_{\frac{\lambda}{2}\psi}((\alpha_i + \gamma_i^t)/2) \right)_{1 \leq i \leq L},$$

$$\mathcal{P}_{\mathcal{C}'} = \text{prox}_{\mathcal{C}'} = c^{-1}\Phi^T \circ \mathcal{P}_{\mathcal{C}} \circ \Phi + (\mathbf{I} - c^{-1}\Phi^T \circ \Phi)$$

and $\mathcal{P}_{\mathcal{C}}$ is the projector onto the positive orthant $(\mathcal{P}_{\mathcal{C}}\eta)_i = \max(\eta_i, 0)$. Then,

$$\gamma^t \rightharpoonup \gamma \text{ and } \text{prox}_{f_2}(\alpha) = \mathcal{P}_{\mathcal{C}'}(\gamma). \quad (11)$$

We are now ready to state our main proximal iterative algorithm to solve the minimization problem $(P_{\lambda, \psi})$:

Theorem 1. *For $t \geq 0$, let $(\mu_t)_t$ be a sequence in $]0, +\infty[$ such that $0 < \inf_t \mu_t \leq \sup_t \mu_t < (\frac{3}{2})^{3/2} / (2A \|H\|_2^2 \|z\|_\infty)$. Fix $\alpha_0 \in \mathcal{H}$, for every $t \geq 0$, set*

$$\alpha_{t+1} = \text{prox}_{\mu_t f_2}(\alpha_t - \mu_t (\nabla f_1(\alpha_t))) \quad (12)$$

where ∇f_1 and $\text{prox}_{\mu_t f_2}$ are given by Lemma 1 and 2. Then $(\alpha_t)_{t \geq 0}$ converges (weakly) to a solution of $(P_{\lambda, \psi})$.

Proof: We give a sketch of the proof. The main theorem on the proximal iteration can be found in [5, Theorem 3.4]. Hence, combining this theorem with Lemma 1, Lemma 2 and Proposition 1, the result follows. \blacksquare

Note that if the PSF h is low-pass normalized to a unit sum, then $\|H\|_2^2 = 1$.

We now turn to $\text{prox}_{\delta\psi}$ which is given by the following result:

Theorem 2. *Suppose that ψ satisfies, (i) ψ is convex even-symmetric, non-negative and non-decreasing on $[0, +\infty)$, and $\psi(0) = 0$. (ii) ψ is twice differentiable on $\mathbb{R} \setminus \{0\}$. (iii) ψ is continuous on \mathbb{R} , it is not necessarily smooth at zero and admits a positive right derivative at zero $\psi'_+(0) = \lim_{h \rightarrow 0^+} \frac{\psi(h)}{h} > 0$. Then, the proximity operator $\text{prox}_{\delta\psi}(\beta) = \hat{\alpha}(\beta)$ has exactly one continuous solution decoupled in each coordinate β_i :*

$$\hat{\alpha}_i(\beta_i) = \begin{cases} 0 & \text{if } |\beta_i| \leq \delta\psi'_+(0) \\ \beta_i - \delta\psi'(\hat{\alpha}_i) & \text{if } |\beta_i| > \delta\psi'_+(0) \end{cases} \quad (13)$$

A proof of this theorem can be found in [11]. Among the most popular penalty functions ψ satisfying the above requirements, we have $\psi(\alpha_i) = |\alpha_i|$, in which case the associated proximity operator is soft-thresholding. In this case, iteration (12) is essentially an iterative thresholding algorithm with a positivity constraint.

5. EXPERIMENTAL RESULTS

The performance of our approach has been assessed on several 2D datasets, from which we here illustrate two examples. Our algorithm was compared to RL without regularization, RL with multi-resolution support wavelet regularization [2, RL-MRS], the naive proximal method that would assume the noise to be Gaussian (NaiveGauss), and the approach of [9] (AnsGauss). For all results presented, each algorithm was run with 200 iterations, except RL which was stopped when its MSE was smallest.

In Fig.1, the original Lena image with a maximum intensity of 30 is depicted in (a), its blurred and blurred+noisy versions are in (b) and (c). With Lena, and for NaiveGauss, AnsGauss and our approach, the dictionary Φ contained the curvelet tight frame. The deconvolution results are shown in Fig.1(d)-(h). As expected, the RL is the worst as it lacks regularization. There are also noticeable artifacts in NaiveGauss, AnsGauss and RL-MRS. Our deconvolved image appears much cleaner. This visual impression is confirmed by quantitative measures of the quality of deconvolution, where we used both the mean ℓ_1 -error (adapted to Poisson noise), and the well-known MSE criteria. The mean ℓ_1 -error for Lena is shown in Tab.1 (similar results were obtained for the MSE). In general, our approach performs very well. At low intensity levels, RL-MRS has the smallest error very comparable to our approach. For the other intensity levels, our algorithm provides the best performance. At high intensity levels, NaiveGauss is competitive. This comes as no surprise since this is an intensity regime where Poisson noise approaches the Gaussian behavior. On the other hand, the results reveal that AnsGauss performs poorly just after RL, probably because it does not handle properly the non-linearity of the degradation model (2) after the VST.

We further illustrate the capabilities of our approach on a confocal microscopy simulation. We have created a phantom of an image of a neuron dendrite segment with a mushroom-shaped spines, see Fig.2. The experimental settings were the same as for Lena except that the dictionary here contained the wavelet transform. The findings are similar to those of Lena both visually and quantitatively.

Method	Intensity regime			
	≤ 5	≤ 30	≤ 100	≤ 255
Our method	0.39	0.93	2.63	7.21
NaiveGauss	0.59	1.65	3.56	6.9
AnsGauss	0.87	2.33	4.61	8.35
RL-MRS	0.35	1.76	4.31	9.5
RL	1.97	5.07	9.53	15.68

Table 1. Mean ℓ_1 -error of all algorithms as a function of the intensity level.

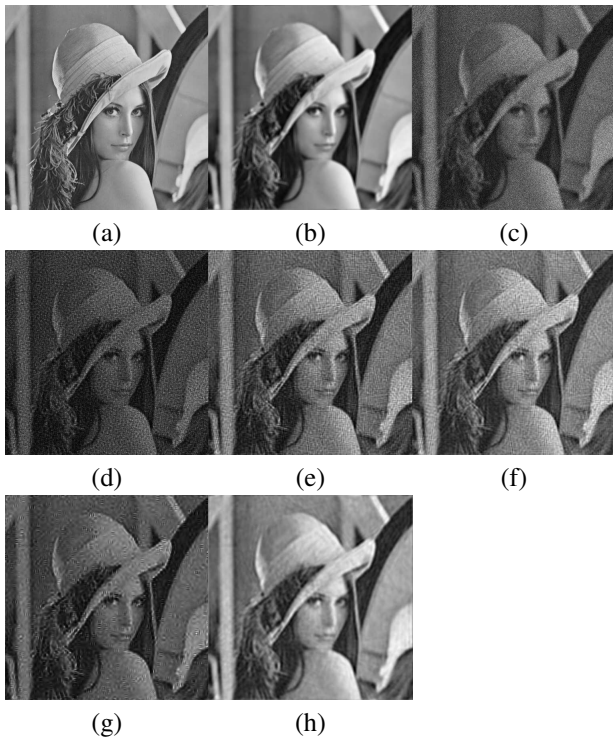


Fig. 1. Deconvolution of Lena. (a) Original, (b) Blurred, (c) Blurred+noisy, (d) RL, (e) NaiveGauss, (f) AnsGauss, (g) RL-MRS, (h) Our algorithm.

6. CONCLUSION

In this paper, we presented a sparsity-based fast iterative thresholding deconvolution algorithm that takes account of the presence of Poisson noise. A careful theoretical characterization of the algorithm and its solution is provided. The encouraging experimental results clearly confirm the capabilities of our approach.

7. REFERENCES

- [1] P. Sarder and A. Nehorai, "Deconvolution Method for 3-D Fluorescence Microscopy Images," *IEEE Sig. Pro.*, vol. 23, pp. 32–45, 2006.
- [2] J.-L. Starck and F. Murtagh, *Astronomical Image and Data Analysis*, Springer, 2006.
- [3] N. Dey, L. Blanc-Fraud, C. Zimmer, Z. Kam, J.-C. Olivo-Marin, and J. Zerubia, "A deconvolution method for confocal microscopy with total variation regularization," in *IEEE ISBI*, 2004.
- [4] I. Daubechies, M. Defrise, and C. De Mol, "An iterative thresholding algorithm for linear inverse problems with a sparsity constraints," *Comm. Pure Appl. Math.*, vol. 112, pp. 1413–1541, 2004.
- [5] P. L. Combettes and V. R. Wajs, "Signal recovery by proximal forward-backward splitting," *SIAM MMS*, vol. 4, no. 4, pp. 1168–1200, 2005.
- [6] G. Teschke, "Multi-frame representations in linear inverse problems with mixed multi-constraints," *ACHA*, vol. 22, no. 1, pp. 43–60, 2007.

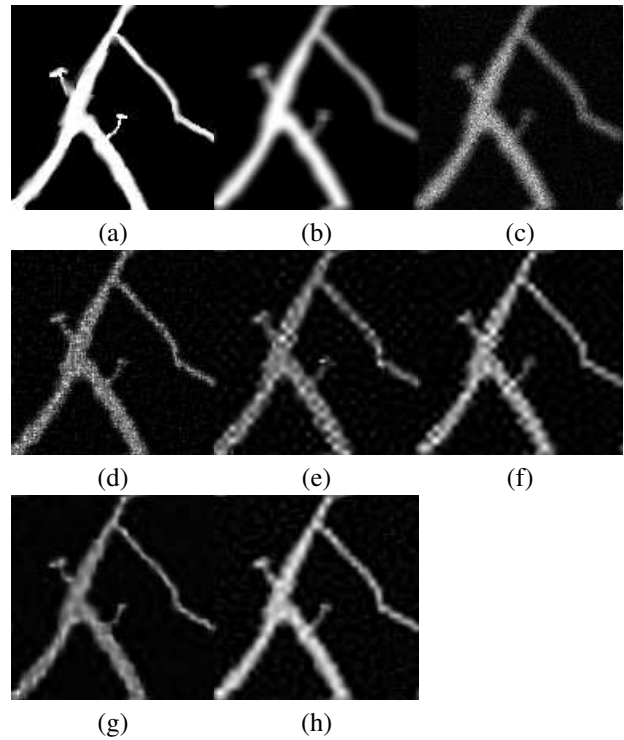


Fig. 2. Deconvolution of Neuron image. (a) Original, (b) Blurred, (c) Blurred+noisy, (d) RL (mean ℓ_1 -error 2.1841), (e) NaiveGauss (1.6368), (f) AnsGauss (2.0477), (g) RL-MRS (1.1926), (h) Our algorithm (1.335).

- [7] C. Chau, P. L. Combettes, J.-C. Pesquet, and V. R. Wajs, "A variational formulation for frame-based inverse problems," *Inv. Prob.*, vol. 23, pp. 1495–1518, 2007.
- [8] M. J. Fadili and J.-L. Starck, "Sparse representation-based image deconvolution by iterative thresholding," in *ADA IV*, France, 2006, Elsevier.
- [9] C. Chau, L. Blanc-Féraud, and J. Zerubia, "Wavelet-based restoration methods: application to 3d confocal microscopy images," in *SPIE Wavelets XII*, 2007.
- [10] J.-J. Moreau, "Fonctions convexes duales et points proximaux dans un espace hilbertien," *CRAS Sér. A Math.*, vol. 255, pp. 2897–2899, 1962.
- [11] M.J. Fadili, J.-L. Starck, and F. Murtagh, "Inpainting and zooming using sparse representations," *The Computer Journal*, 2006, in press.